Front. Optoelectron. 2019, 12(2): 180–189
https://doi.org/10.1007/s12200-018-0818-9

RESEARCH ARTICLE

Shape reconstruction of large optical surface with high-order terms in fringe reflection technique

Xiaoli JING[1,2], Haobo CHENG (✉)[1,2], Yongfu WEN (✉)[1,2]

1 School of Optics and Photonics, Beijing Institute of Technology, Beijing 100081, China
2 Shenzhen Research Institute, Beijing Institute of Technology, Shenzhen 518057, China

Abstract A fast and effective shape reconstruction method of large aspheric specular surfaces with high order terms is proposed in fringe reflection technique, which combines modal estimation with high-order finite-difference algorithm. The iterative equation with high-order truncation errors is derived for calculating the specular surface with large aperture based on high-order finite-difference algorithm. To achieve the wavefront estimation and improve convergence speed, the numerical orthogonal transformation method based on Zernike polynomials is implemented to obtain the initial iteration value. The reconstruction results of simulated surface identified the advantages of the proposed method. Furthermore, a freeform in illuminating system has been used to demonstrate the validity of the improved method in practical measurement. The results show that the proposed method has the advantages of making the reconstruction of different shape apertures accurate and rapid. In general, this method performs well in measuring large complex objects with high frequency information in practical measurement.

Keywords shape reconstruction, fringe reflection technique, Zernike orthogonal transformation, finite difference, measurement

1 Introduction

The core idea in fringe reflection technique is that mirroring patterns are distorted depending on the shape of the object [1], providing a direct measurement of discrete slope variations [2]. A process to reconstruct the surface shape from the gradient data are consequently required. Huang et al. [3] divided the integration methods into three categories. The first category is the finite-difference based least-squares integration (FLI) methods. The zonal reconstruction approach with three different kinds of grid sampling configurations [4–6] are common types. To reconstruct the high order components for improving accuracy, Huang and Asundi [7] used an iterative compensation algorithm and Li et al. [8] applied the high-order finite-difference algorithm in the Southwell grid. Zhou et al. [2] combined the Legendre polynomials method and Southwell zonal reconstruction (SZR) algorithm to improve the convergent speed. The second category of integration methods is the transform-based integration (TI) methods. The discrete Fourier transform [9,10] and discrete cosine transform-based methods [3] were employed to reconstruct the wavefront by integrating the multiple directional derivatives. The integration from only one partial derivative in the Fourier domain is simple and fast with the priori knowledge of the characteristics of the test object [11]. The third one is the radial basis function based integration (RBFI) method. Besides, Ettl et al. [12] introduced an integration method by employing the radial basis functions, and Bon et al. [13] proposed a boundary Fourier integration method by simply padding slope matrices with positive or negative slope values. Traditional cross-path integration is easy to implement and very efficient in computing speed [14] with relatively low accuracy. Recently, we presented a quality map path integration method [15], which reconstructs the surface by using a quality map to guide the path integration. It should be noted that the high-order finite-difference algorithm is usually used to achieve the reconstruction for optical surface with higher than third-order terms. The iterative equations are derived by us considering the computational memory for large aspheric surface. However, the convergence for computing height from a large data sets is very

Received April 4, 2018; accepted July 11, 2018

E-mails: chenghaobo@tsinghua.org.cn, yf_wen@126.com

slow, and the stability is poor in conditions of strong noise.

In this paper, we concentrate on an improved method with fast speed and high accuracy in practical measurement of fringe reflection technique over different apertures and shapes. The orthogonal polynomials based on Zernike polynomials are used here to calculate the initial height of iterative process. Thus the proposed method combined the advantages of both modal and zonal estimation approaches, making it possible to reconstruct the surface shape with high convergent speed. Meanwhile, it can handle the surfaces with different shape apertures. The rest of paper is organized as follows. Section 2 illustrates the principle of traditional reconstruction method and the proposed method. In Section 3, reconstruction simulations with different apertures and shape are conducted, and the performance of the presented method is discussed, demonstrated and verified by examples. Section 4 shows the results of experiment about a freeform surface in illuminating system. Section 5 concludes the work.

2 Reconstruction method

Wavefront reconstruction of surface shape from slopes is a mathematical integration process. First, it is necessary to recall the traditional least-squares integration with Southwell grid model. Then, we propose a method combined the zonal reconstruction method and modal estimation, which performs well in large optical surface with high-order terms.

2.1 Traditional reconstruction algorithm over large optical surface

The appropriate grid pattern for reconstructing the wavefront from the local slopes was first introduced by Southwell. Southwell's zonal wavefront reconstruction algorithm is based on the assumption that the points for height estimation are at the same locations of those whose gradient data has been measured out. The relationship between slope and shape can be expressed as

$$\begin{cases} \dfrac{p_{i+1,j}+p_{i,j}}{2}=\dfrac{z_{i+1,j}-z_{i,j}}{b},\ i=1,2,...,M-1;\ j=1,2,...,N, \\ \dfrac{q_{i,j+1}+q_{i,j}}{2}=\dfrac{z_{i,j+1}-z_{i,j}}{b},\ i=1,2,...,M;\ j=1,2,...,N-1, \end{cases} \tag{1}$$

where $z_{i,j}$ represents the height value at point (i, j), b is the distance between two adjacent grid points, M and N are the number of the grid points in the x and y directions. Furthermore, Eq. (1) can be rewritten in terms of matrices as

$$\boldsymbol{DZ}=\boldsymbol{G}, \tag{2}$$

where

$$\boldsymbol{D}=\begin{bmatrix} -1 & 0 & ... & 1 & 0 & ... & 0 & 0 & 0 & ... & ... & 0 \\ 0 & -1 & 0 & ... & 1 & 0 & ... & 0 & 0 & 0 & ... & 0 \\ \vdots & \vdots & \vdots & \vdots & \vdots & \vdots & \vdots & \vdots & \vdots & \vdots & \vdots & \vdots \\ 0 & ... & ... & ... & ... & ... & ... & 0 & -1 & 0 & ... & 1 \\ -1 & 1 & 0 & ... & ... & ... & ... & ... & ... & ... & ... & 0 \\ 0 & -1 & 1 & 0 & ... & ... & ... & ... & ... & ... & ... & 0 \\ \vdots & \vdots & \vdots & \vdots & \vdots & \vdots & \vdots & \vdots & \vdots & \vdots & \vdots & \vdots \\ 0 & ... & ... & ... & ... & ... & ... & ... & ... & 0 & -1 & 1 \end{bmatrix}_{[(M-1)N+M(N-1)]\times MN},$$

$$\boldsymbol{z}=\begin{bmatrix} z_{1,1} \\ z_{2,1} \\ \vdots \\ z_{M,N} \end{bmatrix}_{MN\times 1},\ \boldsymbol{G}=\frac{1}{2}\begin{bmatrix} (p_{1,2}+p_{1,1})(x_{1,2}-x_{1,1}) \\ (p_{1,3}+p_{1,2})(x_{1,3}-x_{1,2}) \\ \vdots \\ (p_{M,N}+p_{M,N-1})(x_{M,N}-x_{M,N-1}) \\ (q_{2,1}+q_{1,1})(y_{2,1}-y_{1,1}) \\ (q_{3,1}+q_{2,1})(y_{3,1}-y_{2,1}) \\ \vdots \\ (q_{M,N}+q_{M-1,N})(y_{M,N}-y_{M-1,N}) \end{bmatrix}_{[(M-1)\times N+M(N-1)]\times 1}. \tag{3}$$

Therefore, the least-squares norm solution can be obtained by Eq. (4):

$$\boldsymbol{Z} = \boldsymbol{D}^{+}\boldsymbol{G}, \tag{4}$$

where $\boldsymbol{D}^{+}$ is the generalized inverse matrix of $\boldsymbol{D}$ and is a sparse matrix. When the matrix size is smaller, Eq. (4) can achieve the height information quickly and precisely. But it will take up large amounts of memory when the matrix size is larger. So an iteration strategy is used to handle larger matrix based on Eq. (4), which is described as

$$z_{i,j}^{(m+1)} = \overline{z}_{i,j}^{(m)} + b_{i,j}/g_{i,j}, \tag{5}$$

where

$$\begin{aligned} \overline{z}_{i,j} &= (z_{i+1,j} + z_{i-1,j} + z_{i,j+1} + z_{i,j-1})/g_{i,j}, \\ b_{i,j} &= (p_{i+1,j} - p_{i-1,j} + q_{i,j+1} - q_{i,j-1})b/2, \end{aligned} \tag{6}$$

where $\overline{z}_{i,j}(m)$ is the nearest-neighbor height average after the mth iteration and $b_{i,j}$ is a constant depending only on the gradient measurement data. $z_{i,j}^{(m+1)}$ is the height value after $(m+1)$th iteration; The factor $g_{i,j}$ is either two, three, or four according to whether its corresponding reconstruction height $z_{i,j}$ is on a corner, an edge, or an interior reconstruction point. At the boundary, the corresponding values of height and slope element are assumed to be zero and the negative of the adjacent slope respectively. By utilizing the iterative method, the slopes can be integrated to give the surface map of the tested object.

2.2 Improved reconstruction method for large optical surface with high-order terms

The zonal wavefront reconstruction approach shows slow convergence when dealing with large gradient measurements, even the reconstruction process might fail because the gradient measurements are much smaller than the corresponding height values. Therefore, a rapid and accurate reconstruction method over large specular surface with high-order items is proposed as follows. The proposed method uses the height information calculated by orthogonal Zernike polynomials as initial iteration values first, and then achieves the reconstruction by iteration process based on high-order finite-difference method. Our method aims to combine the advantage of orthogonal Zernike polynomials and high-order finite-difference method, making it possible to reconstruct the 3-D shape of large surfaces with high-order items accurately and rapidly.

Li et al. [8] proposed high-order finite-difference method based on the Taylor theorem to derive the integration equations with different truncation errors. It is considered that the integration equations with smaller truncation errors will improve the reconstruction accuracy. The iteration equations are derived by us in this section. The height information can be acquired as

$$\begin{aligned} z_{i,j+1} - z_{i,j} &= \frac{13h}{24}\left(-\frac{1}{13}p_{i,j-1} + p_{i,j} + p_{i,j+1} - \frac{1}{13}p_{i,j+2}\right), \\ & \qquad i = 1,2,...,M;\ j = 2,3,...,N-1, \\ z_{i+1,j} - z_{i,j} &= \frac{13h}{24}\left(-\frac{1}{13}q_{i-1,j} + q_{i,j} + q_{i+1,j} - \frac{1}{13}q_{i+2,j}\right), \\ & \qquad i = 2,3,...,M-1;\ j = 1,2,...,N. \end{aligned} \tag{7}$$

And the Simpson integration equations were obtained from the head and the end of each row and each column as

$$\begin{aligned} z_{i,j+2} - z_{i,j} &= \frac{h}{3}(p_{i,j} + 4p_{i,j+1} + p_{i,j+2}), \\ & \qquad i = 1,2,...,N;\ j = 1,N-2, \\ z_{i+2,j} - z_{i,j} &= \frac{h}{3}(q_{i,j} + 4q_{i+1,j} + q_{i+2,j}), \\ & \qquad i = 1,N-2;\ j = 1,2,...,N. \end{aligned} \tag{8}$$

The coefficient matrix composed of Eqs. (7) and (8) is sparse matrix, and the calculation will be harder with the increasing size of slope data. Therefore, we proposed the iteration equation based on Eqs. (7) and (8), which can be applied in conditions of handling large data sets. They can be rewritten

$$z_{i,j} = \overline{z}_{i,j} + c_{i,j}, \tag{9}$$

where $\overline{z}_{i,j}$ and $c_{i,j}$ of Eq. (9) are derived as Eqs. (10) and (11), respectively.

$$\begin{aligned} \overline{z}_1|_{i,j} &= \frac{1}{4}(z_{i,j-1} + z_{i,j+1} + z_{i-1,j} + z_{i+1,j}), \\ c_1|_{i,j} &= \frac{13h}{96}\Bigg[-\frac{1}{13}(p_{i,j-2} + p_{i,j+2} + q_{i-2,j} + q_{i+2,j}) \\ & \quad + \frac{12}{13}(p_{i,j-1} + p_{i,j+1} + q_{i-1,j} + q_{i+1,j}) \\ & \quad + 2(p_{i,j} + q_{i,j})\Bigg], \end{aligned} \tag{10}$$

$$\overline{z}_2|_{i,j} = (z_{i,j-2} + z_{i,j+2} + z_{i-2,j} + z_{i+2,j})/g_{i,j},$$

$$c_2|_{i,j} = 4(p_{i,j-1} + p_{i,j+1} + q_{i-1,j} + q_{i+1,j})/g_{i,j}, \tag{11}$$

where $g_{i,j}$ is the same factor in Eq. (5). Therefore, higher order integration method can be transformed in iteration expression at the mth iteration:

$$z_{i,j}^{(m+1)} = \overline{z}_{i,j}^{(m)} + c_{i,j}, \tag{12}$$

where $\overline{z}_{i,j}^{(m)}$ is the height average after the mth iteration, and $z_{i,j}^{(m+1)}$ is the height value after $(m+1)$th iteration. The successive over-relaxation (SOR) method is adopted during the process of iteration, and Eq. (12) can be written by introducing the relaxation parameter ω:

$$z_{i,j}^{(m+1)} = z_{i,j}^{(m)} + \omega\left[\overline{z}_{i,j}^{(m)} + c_{i,j} - z_{i,j}^{(m)}\right], \tag{13}$$

where ω is the relaxation factor to reduce the approximation error faster and is usually chosen as [2]

$$\omega = \frac{2}{1+\sin[\pi/(N+1)]}. \tag{14}$$

However, the convergence for the iteration process from a large or strongly curved gradient field is very slow. Considering the acceleration of online processing speed, numerical orthogonal gradient and surface polynomials based on Zernike polynomials [16] are used to calculate the initial value here, which can be employed in the wavefront estimation over different shaped apertures. The freeform surface can be expressed based on Zernike circle polynomials as

$$F_l(x,y) = \sum_{j=1}^{J} C_{lj} Z_j(x,y), \tag{15}$$

where $F_l(x,y)$ is freeform surface, C_{lj} is the transform coefficient and J is the number of Zernike circle polynomials denoted by Z. The partial derivatives of $F_l(x,y)$ in x and y directions are

$$F_l^x = \frac{\partial F_l(x,y)}{\partial x} = \sum_{j=1}^{J} C_{lj}\frac{\partial Z_j(x,y)}{\partial x} = \sum_{j=1}^{J} C_{lj} Z_j^x,$$

$$F_l^y = \frac{\partial F_l(x,y)}{\partial y} = \sum_{j=1}^{J} C_{lj}\frac{\partial Z_j(x,y)}{\partial y} = \sum_{j=1}^{J} C_{lj} Z_j^y. \tag{16}$$

The first term of Zernike polynomials is constant, then both the first term of F_l^x, F_l^y are zeros. F_l^x, F_l^y are used as numerical basis functions to construct the numerical orthogonal gradient polynomials except the first terms:

$$G_i^x = \sum_{j=2}^{J} D_{il} F_l^x,\ G_i^y = \sum_{j=2}^{J} D_{il} F_l^y. \tag{17}$$

The basis function of freeform surface and gradient data can be expressed:

$$\tilde{\boldsymbol{F}} = \begin{pmatrix} F^x \\ F^y \end{pmatrix} = \begin{pmatrix} Z^x \\ Z^y \end{pmatrix} \boldsymbol{M}^{\mathrm{T}} = \tilde{\boldsymbol{Z}}\tilde{\boldsymbol{M}}^{\mathrm{T}},$$

$$\tilde{\boldsymbol{G}} = \begin{pmatrix} G^x \\ G^y \end{pmatrix} = \begin{pmatrix} \tilde{F}^x \\ \tilde{F}^y \end{pmatrix} \boldsymbol{M}^{\mathrm{T}} = \tilde{\boldsymbol{F}}\boldsymbol{D}^{\mathrm{T}}, \tag{18}$$

where $\tilde{\boldsymbol{M}}^{\mathrm{T}}$, $\boldsymbol{D}^{\mathrm{T}}$ are transposed transformation matrix, and they can be obtained by Gram-Schmidt orthogonal method:

$$\boldsymbol{M} = (\boldsymbol{Q}^{\mathrm{T}})^{-1},\ \boldsymbol{D} = (\boldsymbol{R}^{\mathrm{T}})^{-1}, \tag{19}$$

where

$$\boldsymbol{Q}^{\mathrm{T}}\boldsymbol{Q} = \boldsymbol{Z}^{\mathrm{T}}\boldsymbol{Z}/N,\ \boldsymbol{R}^{\mathrm{T}}\boldsymbol{R} = \tilde{\boldsymbol{F}}^{\mathrm{T}}\tilde{\boldsymbol{F}}/(N+N), \tag{20}$$

where N is the number of data points. In practical measurement, the coefficient matrix $\boldsymbol{\alpha}$ can be calculated based on basis functions in Eq. (18), which can be expressed as

$$\boldsymbol{\alpha} = \begin{pmatrix} G_x \\ G_y \end{pmatrix}^{-1} P, \tag{21}$$

where P is the slope data obtained in the measurement. Then the coefficient matrix $\boldsymbol{\beta}$ is

$$\boldsymbol{\beta} = \boldsymbol{D}^{\mathrm{T}}\hat{\boldsymbol{\alpha}}. \tag{22}$$

3 Simulations

We will perform the shape reconstruction simulations of three different objects to prove the validity of modal wavefront estimation, iterative high-order finite-difference method and our proposed method. The first simulation is used to demonstrate the performance of modal wavefront estimation over different shape apertures, and the second simulation is used to demonstrate the accuracy and speed of high-order finite-difference method. The last simulation demonstrates the advantage of our proposed method on the accuracy and calculating time.

3.1 Reconstruction of hexagon optical surface by orthogonal Zernike polynomials

Consider a freeform surface with hexagon aperture to be measured that is expressed as

$$z(x,y) = 0.5x^2 - 0.3\Big[2(1-x)^2 \mathrm{e}^{-x^2-(y+1)^2} - 10\Big(\frac{x}{5} - x^3 - y^5\Big)\mathrm{e}^{-x^2-y^2} + \frac{1}{3}\mathrm{e}^{-(x+1)^2-y^2}\Big]. \tag{23}$$

The range of x and y are set to be $[-1, 1]$ mm and the matrix size is set 500 pixel × 500 pixel. The simulated data are filtered from the rectangular aperture. The surface shape and slope data are shown in Figs. 1 and 2. Gaussian noise with SNR (signal to noise ratio) = 30 in the slope data are added. Reconstruction error map by Legendre polynomials and orthogonal Zernike polynomials are shown in Fig. 3.

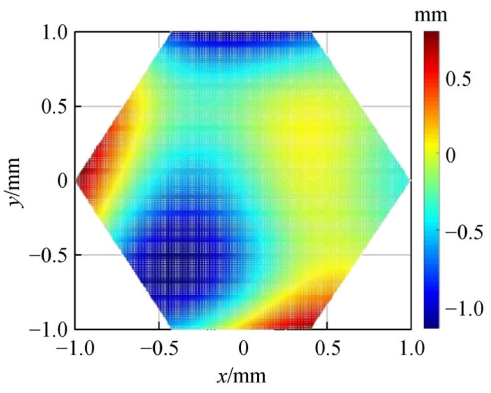

Fig. 1 Surface map of arbitrary surface

Peak-valley (PV) value and root-mean-square (RMS) value of error by orthogonal Zernike polynomials are 4.50 and 0.01 μm, respectively. And PV and RMS by Legendre polynomials are 90 and 8.2 μm. It is clear that when orthogonal Zernike polynomials are applied to the same gradient data with hexagon aperture, the reconstruction shape of high accuracy was achieved, which was much better than the result of Legendre polynomials.

3.2 Reconstruction of freeform surface with high-order terms by iterative high finite-difference method

The freeform surface under simulation is expressed as

$$z = 0.3\cos(0.4x^2 + 2x)\cos(0.4y^2 + 2y) + 0.7\cos[(x^3 + y^2)/(4\pi)]. \quad (24)$$

The range of x and y are set to be $[-5, 5]$ mm and the sample intervals are 0.02 mm. The slope data are shown in Fig. 4. Reconstruction error map by Southwell method, Huang's [7] and iterative high-order finite-difference method are shown in Fig. 5. The corresponding PV value, RMS value and calculating time are listed in Table 1. The results show that iterative high finite-difference method has the highest accuracy, and cost less time than Huang's method.

3.3 Reconstruction of large matrix with high order items

The surface in simulation is an optical surface with high order items as shown

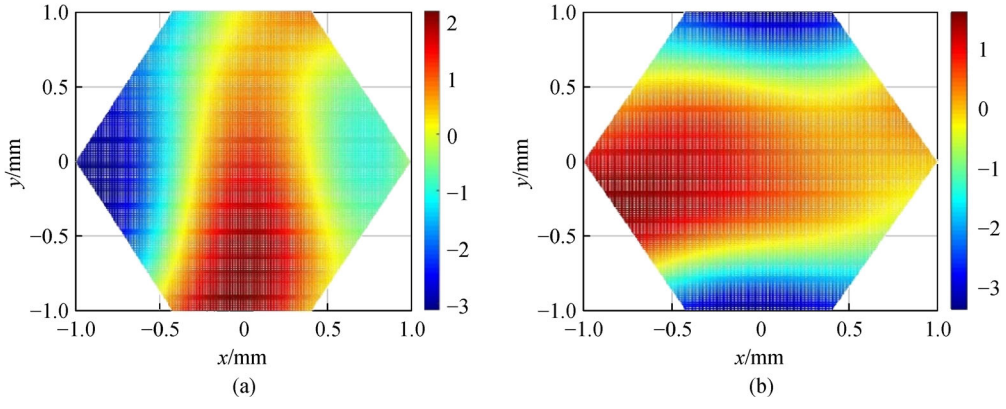

Fig. 2 Slope map of arbitrary surface in (a) x and (b) y direction

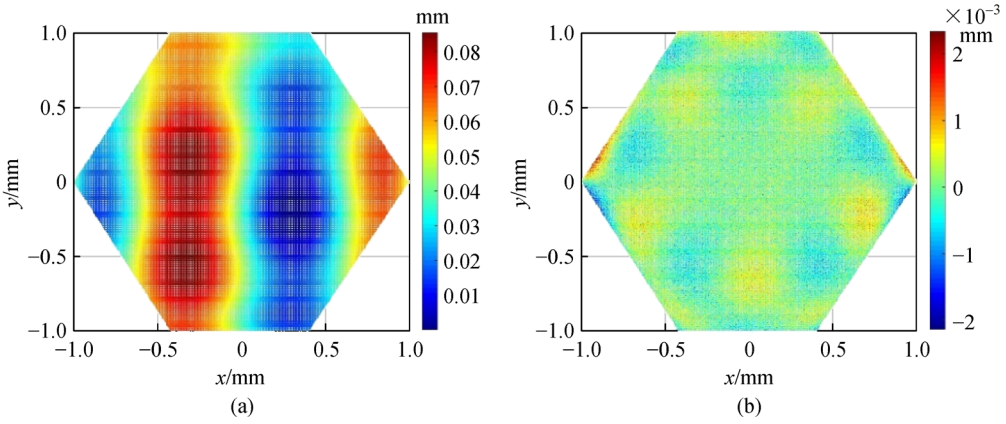

Fig. 3 Reconstruction error by (a) Legendre polynomials and (b) orthogonal Zernike polynomials

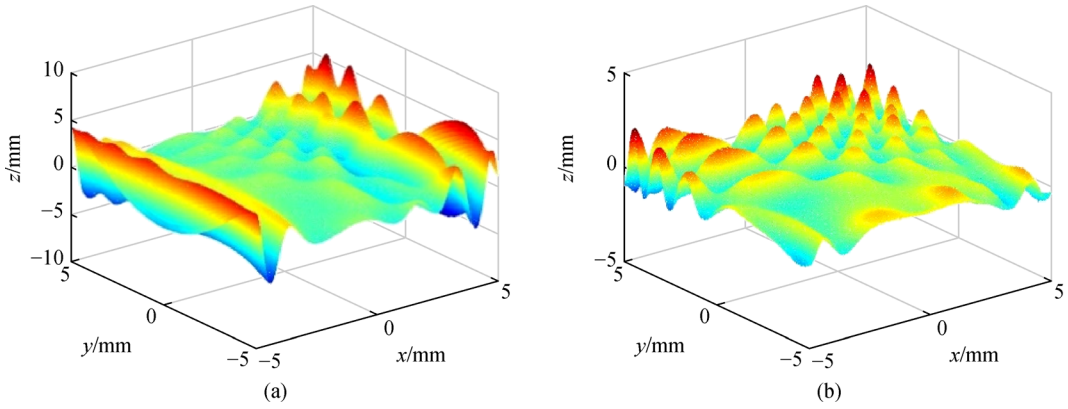

Fig. 4 Slope map of freeform surface in (a) x and (b) y direction

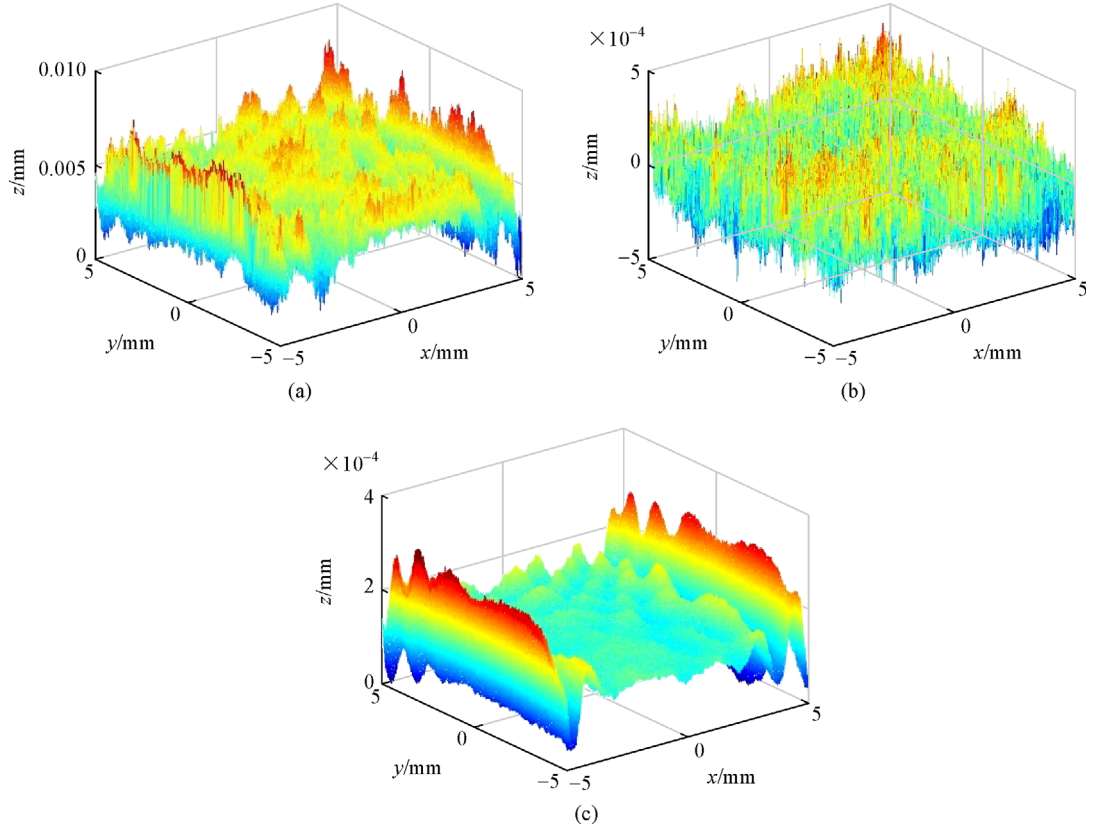

Fig. 5 Error map by (a) Southwell method, (b) Huang's and (c) iterative high-order finite-difference method

Table 1 Analysis of 3D reconstruction results with three methods

reconstruction method	PV/μm	RMS/μm	time/s
Southwell iteration	8.4	4.4	125
Huang's	8.68×10^{-1}	9.72×10^{-2}	152
iterative high finite-difference	3.3×10^{-1}	9×10^{-2}	128

$$z(x,y) = 3\ (1-x)^2 \mathrm{e}^{-x^2-(y+1)^2} - 10\left(\frac{x}{5}-x^3-y^5\right)\mathrm{e}^{-x^2-y^2} - \frac{1}{3}\,\mathrm{e}^{-(x+1)^2-y^2}. \quad (25)$$

The range of x and y are set −5 to 5 mm and the matrix size is set 1000 pixel × 1000 pixel. The shape of these tested surfaces are shown in Fig. 6. Normally distributed noise with SNR = 30 is added to the ideal slopes. The performance about computing time and accuracy using different methods is shown in Table 2. The RMS and PV values of errors characterize the accuracy of reconstructed surface. The error maps are shown in Fig. 7. The arbitrary surface was reconstructed by Southwell iteration method, Zhou's, Huang's, high-order finite-difference method and our method.

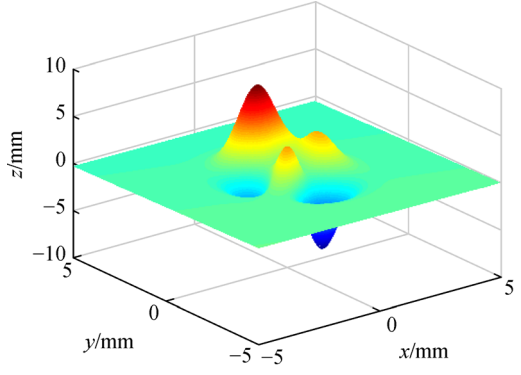

Fig. 6 Shape map of simulated surface

We noticed that Zhou's method performs better in computing speed, and high finite-difference method has better accuracy. When using the proposed method for shape reconstruction, the RMS value realizes 10-fold magnitude improvement and the corresponding computing speed increases by 4-fold compared with the traditional Southwell iteration method. It is apparent from Fig. 7 that, high-order finite-difference method and our method can handle higher-order terms better than Huang's, which has larger error propagation and edge effect. Besides, our method plays an important role in accuracy based on initial value, which is obtained by Legendre polynomials as Fig. 7(e). Therefore, iteration equations based on higher order integration is necessary and important considering the accuracy. To sum up, our method has relatively higher accuracy and faster reconstruction speed, providing an efficient solution for large matrix with high-order terms in fringe reflection technique, which can be used in the reconstruction of large optical surface.

4 Experiment

A freeform optical surface used in illuminating system has been measured, the reconstruction error of the Zernike, Southwell, and our proposed method for circular freeform optical surface are shown in Figs. 8(a)–8(c). Our proposed method reconstructed the surface errors achieved the values of 0.0931 (RMS) and 0.153 (PV) μm, which is shown in Table 3. Compared with the Southwell iteration method, reconstruction accuracy had an order of magnitude higher, and the time was only 18 s. It is apparent from the result that our proposed method has relatively good effect for 3D shape reconstruction, paving the way for engineering application in fringe reflection technique.

5 Conclusion

Generally, a rapid, accurate and easily implemented method is proposed to reconstruct the large optical surface with high-order terms. The merits of proposed method can be summarized as follows. First, the proposed method can be used to reconstruct optical surface with different shape apertures, which expanded the application of 3D reconstruction in fringe reflection technique. Second, our method is good at handing large optical surface with high order terms, still fast as improving the accuracy compared with traditional algorithm. In summary, our method is an effective and accurate tool in practical measurement. The limitation for this proposed method is also investigated. It cannot handle irregular mesh grid very well because of the non-uniform grids, but the rectangular mesh grid is relatively common in practical measurement.

Table 2 Analysis of 3D reconstruction results of measured surfaces under SNR = 30

measured surface	reconstruction method	PV/μm	RMS/μm	time/s
arbitrary	Southwell iteration	2.42	1.44×10^{-1}	125
	Zhou's	1.8	1.12×10^{-1}	26
	Huang's	3.80×10^{-1}	4.08×10^{-2}	141
	Li's	1.48×10^{-1}	1.49×10^{-2}	127
	our	9.6×10^{-2}	1.35×10^{-2}	27

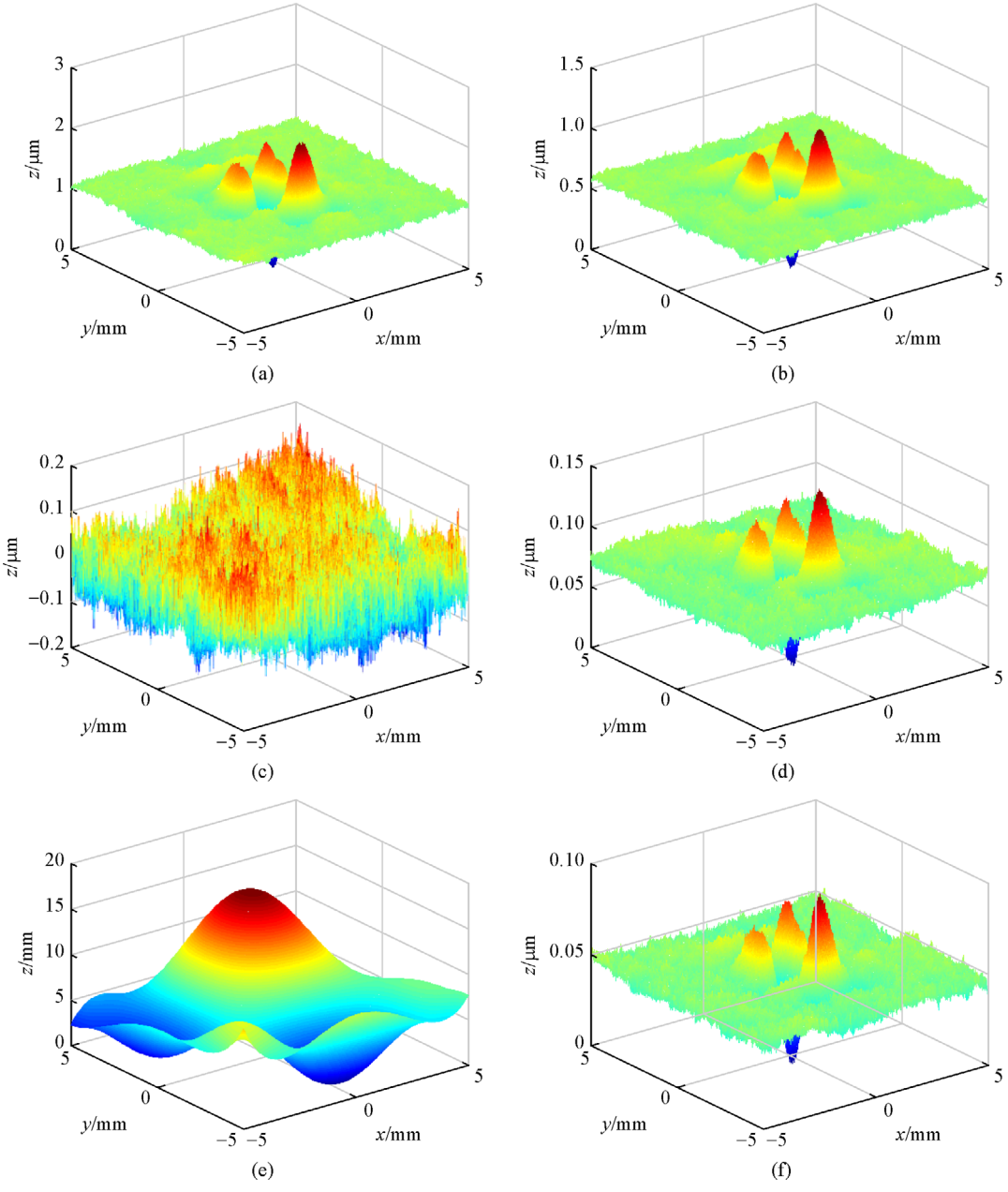

Fig. 7 Absolute errors of arbitrary surface using different methods. (a) SOR method based on Southwell geometry; (b) combined SOR with Legendre method proposed by Zhou; (c) iterative compensation method proposed by Huang; (d) iteration equation based on higher order integration method proposed by Li; (e) Legendre polynomials method; (f) our method

Table 3 Comparison of reconstruction error of freeform surface by two methods

tested surface	reconstruction method	PV/μm	RMS/μm	time/s
arbitrary (800 pixel × 800 pixel)	Southwell iteration	1.42	8.39×10^{-1}	101
	our method	1.53×10^{-1}	9.31×10^{-2}	18

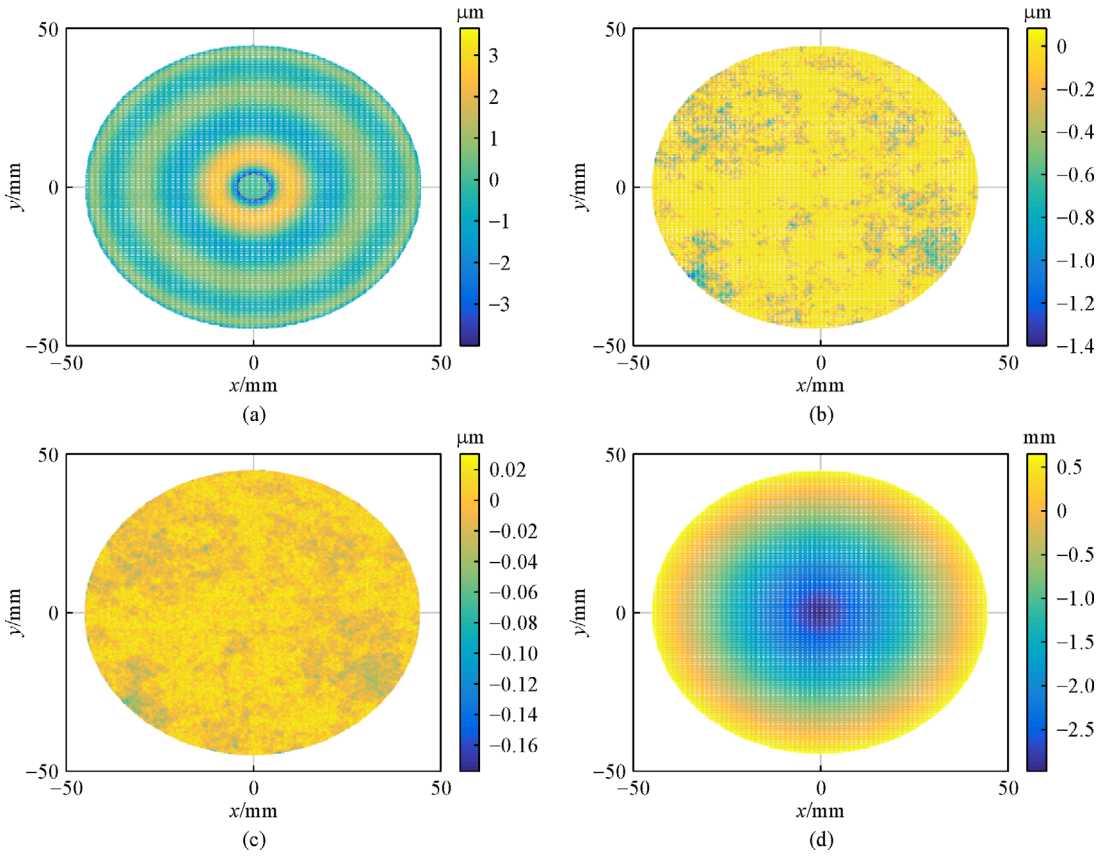

Fig. 8 Error map by (a) Zernike polynomials, (b) Southwell iteration method, (c) our method and (d) reconstructed shape

Acknowledgements The project was supported by Science & Technology Innovation Foundation of Shenzhen (Nos. JCYJ20170817114951575, KQJSCX20160217143907).

References

1. Xiao Y L, Su X, Chen W. Flexible geometrical calibration for fringe-reflection 3D measurement. Optics Letters, 2012, 37(4): 620–622
2. Zhou T, Chen K, Wei H, Li Y. Improved method for rapid shape recovery of large specular surfaces based on phase measuring deflectometry. Applied Optics, 2016, 55(10): 2760–2770
3. Huang L, Idir M, Zuo C, Kaznatcheev K, Zhou L, Asundi A. Comparison of two-dimensional integration methods for shape reconstruction from gradient data. Optics and Lasers in Engineering, 2015, 64: 1–11
4. Hudgin R H. Wave-front reconstruction for compensated imaging. Journal of the Optical Society of America, 1977, 67(3): 375–378
5. Fried D L. Least-square fitting a wave-front distortion estimate to an array of phase-difference measurements. Journal of the Optical Society of America, 1977, 67(3): 370–375
6. Southwell W H. Wave-front estimation from wave-front slope measurements. Journal of the Optical Society of America, 1980, 70 (8): 998–1006
7. Huang L, Asundi A. Improvement of least-squares integration method with iterative compensations in fringe reflectometry. Applied Optics, 2012, 51(31): 7459–7465
8. Li G, Li Y, Liu K, Ma X, Wang H. Improving wavefront reconstruction accuracy by using integration equations with higher-order truncation errors in the Southwell geometry. Journal of the Optical Society of America A, Optics, Image Science, and Vision, 2013, 30(7): 1448–1459
9. Campos J, Yaroslavsky L P, Moreno A, Yzuel M J. Integration in the Fourier domain for restoration of a function from its slope: comparison of four methods. Optics Letters, 2002, 27(22): 1986–1988
10. Bahk S W. Highly accurate wavefront reconstruction algorithms over broad spatial-frequency bandwidth. Optics Express, 2011, 19 (20): 18997–19014
11. Matías Di Martino J, Flores J L, Pfeiffer F, Scherer K, Ayubi G A, Ferrari J A. Phase retrieval from one partial derivative. Optics Letters, 2013, 38(22): 4813–4816
12. Ettl S, Kaminski J, Knauer M C, Häusler G. Shape reconstruction from gradient data. Applied Optics, 2008, 47(12): 2091–2097
13. Bon P, Monneret S, Wattellier B. Noniterative boundary-artifact-free wavefront reconstruction from its derivatives. Applied Optics, 2012, 51(23): 5698–5704
14. Zhang H, Han S, Liu S, Li S, Ji L, Zhang X. 3D shape reconstruction of large specular surface. Applied Optics, 2012, 51(31): 7616–7625
15. Jing X, Cheng H, Wen Y. Path integration guided with a quality map for shape reconstruction in the fringe reflection technique.

Measurement Science & Technology, 2018, 29(4): 045011
16. Ye J, Wang W, Gao Z, Liu Z, Wang S, Benítez P, Miñano J C, Yuan Q. Modal wavefront estimation from its slopes by numerical orthogonal transformation method over general shaped aperture. Optics Express, 2015, 23(20): 26208–26220

Xiaoli Jing is a doctor candidate at Beijing institute of Technology, where she also got her Master degree. Her present research work involves optical measuring.

Haobo Cheng is currently a Professor and doctoral supervisor at the Beijing Institute of Technology. He is also the dean of a research institute in Shenzhen and director of the joint research center for opto-mechatronics engineering. His present research work involves precision and ultra-precision manufacturing and testing.

Yongfu Wen is currently a Master's degree supervisor at the Beijing Institute of Technology. He received his Ph.D. degree at the Beijing Institute of Technology and works at the joint research center for opto-mechatronics engineering. His present research work involves optical measuring and testing.